



Journal of Applied Sciences

ISSN 1812-5654

science
alert

ANSI*net*
an open access publisher
<http://ansinet.com>

A Neutral-Point Voltage Balance Technique for Diode-Clamped Three-level PWM Rectifier Based on Fuzzy Control

¹Yu Fang, ¹Yong Xie and ²Yan Xing

¹College of Information Engineering, Yangzhou University, 225009, Yangzhou, China

²Aero-Power Sic-Tech Center, Nanjing University of Aeronautics and Astronautics, 210016, Nanjing, China

Abstract: The reason why the Neutral Point (NP) voltage unbalance is analyzed in detail, and a Fuzzy Controller based on control index proposed. Fuzzy controller can automatically and intelligently find the value of the control index and adjust the operation time duration of the small vectors. This method for balancing the NP voltage is simple and need not extra hardware cost. In the study, the design method of fuzzy controller has also been presented in details. Finally, the experimental results verify the proposed technique and the balance of the NP voltage guarantees high power factor of TL-PWM rectifier.

Key words: Three-level power converter, balance of neutral-point voltage, fuzzy control, power factor correction, SVPWM

INTRODUCTION

Three-Level (TL) PWM rectifier is much fit to high output voltage and large-scale-power level situation. Especially voltage-type PWM rectifier can work in four quadrants and make power implement bidirectional flow, moreover implement the unity power factor at AC side (Cheng *et al.*, 2008; Kim *et al.*, 2010; Singh and Sharma, 2011; Jiang *et al.*, 2008; Gong *et al.*, 2013; Wang *et al.*, 2011; Qu *et al.*, 2011).

TL converter often produces three kinds of voltage level by virtue of the series electrolytic capacitor at DC side. The balance of neutral-point voltage between the two output capacitors is very important to diode-clamped TL PWM rectifier. How to control it and improve its performance is a research hotspot. If neutral point is unbalanced, low order harmonics will be produced, also the lifetime of the electrolytic capacitor is shortened, so that efficiency of the power converter is degraded and high power factor can not be achieved (Fan, *et al.*, 2012; Song and Feng, 2011; Chen *et al.*, 2012; Yan *et al.*, 2011; Dou *et al.*, 2011; Lan *et al.*, 2011; Rajashekhar and Vittal, 2010; Du *et al.*, 2010).

It is well known that the redundancy small vector can implement the balance in the NP by deciding the time duration of the positive and negative small vector. However, the time duration of the positive and negative small vector commonly is assigned by multiplying constant value called control coefficient. This method may induce the new unbalanced NP voltage and the opposite voltage imbalance across the two electrolytic

capacitors. Hence, the value of the control coefficient needs repetitious experiments. To solve this problem this study proposes the intelligent control method based on fuzzy controller for control coefficient.

The fuzzy control of the control coefficient can intelligently decide the time duration of the positive and negative small vector in light of the grade of the unbalanced NP voltage, so that the voltage of the two capacitors can reach to the same perfectly. The experimental prototype is tested and the experimental results show that the control coefficient based on the fuzzy controller guarantees the NP balance, the steady and the dynamic characteristic and high power factor of TL-PWM rectifier.

NEUTRAL POINT VOLTAGE IMBALANCE

As shown in Fig. 1 is the main circuit of the TL diode-clamped PWM rectifier. There are main two reasons why the two capacitors are unbalanced. The first is caused by the disagreement of the switches parameters; the second is made by the structure of TL converter itself. Both reasons are impersonal existence and solved only by control algorithm.

Unbalance of the neutral-point voltage: With assumption the voltages of the output capacitors equal $u_{dc}/2$. As shown in Fig. 2, the neutral-point voltage should be influenced by output current i_o , the expression is shown in Eq. 1:

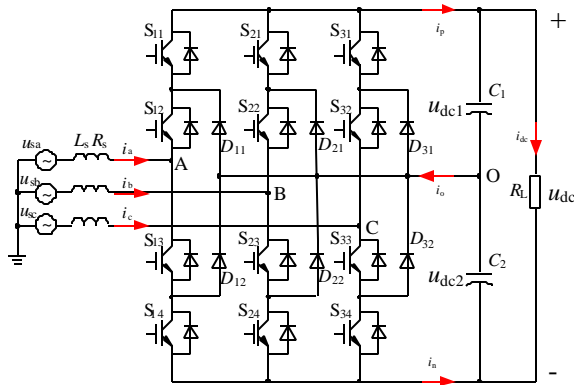


Fig.1: The main circuit of tree-level PWM rectifier

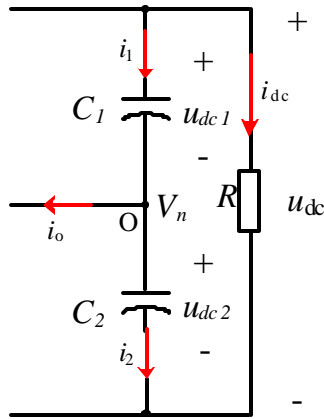


Fig. 2: Neutral-point voltage of the balanced capacitor

$$\begin{cases} i_1 = C_1 \frac{d(u_{dc}/2 - V_n)}{dt} \\ i_2 = C_2 \frac{d(V_n - u_{dc}/2)}{dt} \\ i_o = i_1 - i_2 = -2C_s \frac{dV_n}{dt} \end{cases} \quad (1)$$

From the Eq. 1, we can get:

$$\frac{dV_n}{dt} = -\frac{i_o}{2C_s} \quad (2)$$

Figure 2 shows that the neutral-point voltage V_n varies with i_o .

The unbalance of the NP voltage induced by general SVM is analyzed below.

Three-level PWM rectifier have three bridge legs and each leg has three kinds of states, so there are twenty seven kinds of states altogether. Among these states

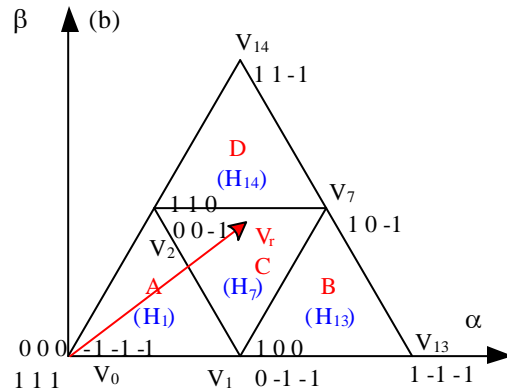
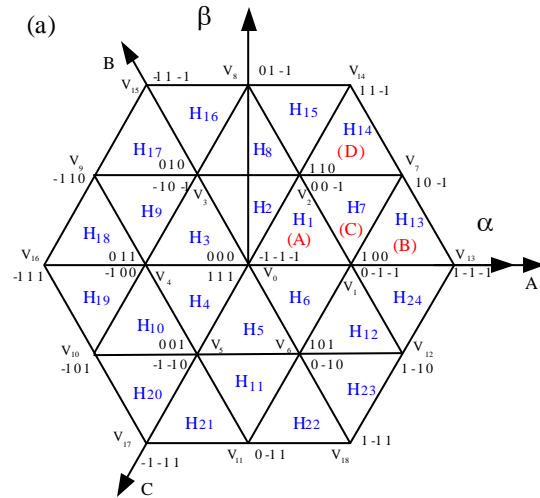


Fig. 3(a-b): Space vector diagram (a) Voltage space vector and (b) The vectors in sector 1

there are twenty four kinds of nonzero vectors and three kinds of zero vectors. In light of the norm of the vector, these voltage vectors can be put into four categories: zero vector, small vector, medium vector and large vector. It is obvious that zero vectors can not affect the NP voltage. Figure 3 is voltage space vector diagram.

First, when large vector works, three-phase input power supply does not connect neutral point O and C_1 together with C_2 locates one circuit, hence two output capacitors charge or discharge at the same time and the voltage of the output capacitor is equal. And thus large vector does not influence the voltage balance of the capacitor.

Second, when medium vector works, C_1 and C_2 charge or discharge via three-phase power supply, respectively, i.e., they have their own circuit. Although the average currents of the self-governed circuit equal, the phase difference of charging or discharging currents

between these two circuits exists. As a consequence the voltages of the C_1 and C_2 can not equal. Seen from Fig. 3, we can not use medium vector to balance the voltage of the capacitor because there does not exist redundant medium vector but only one.

And at the last, when small vector works, power supply are connected between the point O and $+$ or O and $-$, i.e., power supply only spans one capacitor. Hence, only one of the output capacitors constructs the charging or discharging circuit together with power supply. The voltage of one capacitor increases because of charging while the voltage of the other capacitor decreases and vice versa. It is clear that the voltage balance of the capacitor is influenced worst in this operating state.

Neutral-point voltage balance controlled by small vectors:

It's seen from Fig. 3a that each small vector has two kinds of implementation method, i.e., small vector is redundant. We define the small vector consisting of zero and high level as positive small vector while the small vector consisting of zero and negative level as negative small vector and use suffix p and n to distinguish them, respectively.

When reference voltage vector V_r in the first sector as shown in Fig. 3b, if the vector $V_{1p}(100)$ is selected, the equivalent circuit can be gotten as shown in Fig. 4a. Here, C_1 is charged while C_2 discharged, as a result u_{dc1} raises and u_{dc2} declines; if the vector $V_{1n}(0-1-1)$ is selected, the equivalent circuit can be gotten as shown in Fig. 4b. Here, C_1 is discharged while C_2 charged, as a result u_{dc1} declines and u_{dc2} rises. It can be concluded that although initially $u_{dc1} = u_{dc2} = u_{dc}/2$, V_{1p} and V_{1n} can make u_{dc1} and u_{dc2} unequal and most of importance, the function of the vector V_{1p} and V_{1n} is opposite.

BASIC OF THE NEUTRAL POINT VOLTAGE BALANCE USING CONTROL COEFFICIENT

The reference positive polarity of neutral-point input current can be defined as shown in Fig. 2, if the current flow from the point O , i_o is positive. If the desired reference voltage vector locates in the area H_{13} , $u_{dc1} - u_{dc2} > h$ (h is the width of hysteresis) and the neutral point current is positive, the time span of the positive small vector as shown in Fig. 4a should be set lower than that of the negative small vector as shown in Fig. 4b. And thus, the average neutral point current flows toward the point O to discharge C_1 and charge C_2 and finally u_{dc1} equals u_{dc2} . In order to implement digital control conveniently, control coefficient ρ is introduced, the time span of the positive small vector and negative one can be regulated by the control coefficient ρ to implement the balance of the neutral point voltage.

The time span of the operation vector can be calculated as follows:

$$\begin{cases} T_a = 0.5\rho(T - T_1 - T_2) \\ T_b = T_a + 0.5T_1 \\ T_c = T_b + 0.5T_2 \end{cases} \quad (3)$$

Table 1 presents the rule for generating vector in the first sector, the other sectors resembles it.

Table 1: Vector sequence in the first sector

Sector	Area		$\rho T_p/2$	$T_1/2$	$T_2/2$	$(1-\rho)T_0$
Sector I	A	A1	POO	OOO	OON	ONN
		A2	PPO	POO	OOO	OON
	B	POO	PON	PNN	ONN	
		C	C1	POO	PON	OON
	D	C2	PPO	POO	PON	OON
		D	PPO	PPN	PON	OON

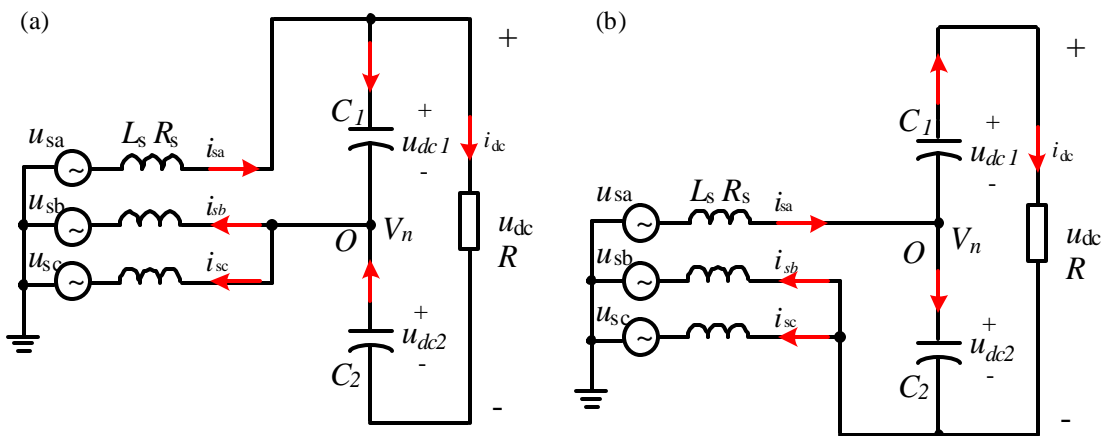


Fig. 4(a-b): Equivalent circuits when V_{1p} and V_{1n} operating, respectively

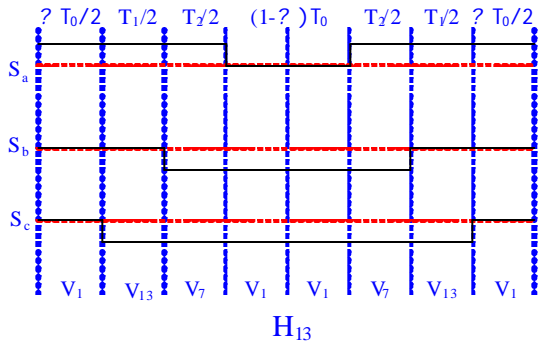


Fig.5: Timing diagram of output voltage vectors

When in the area H_{13} , the concrete timing diagram is shown in Fig. 5 and the drive signals for three-phase bridge legs can be gotten.

DESIGN PRINCIPLE FUZZY CONTROLLER FOR THE CONTROL COEFFICIENT

It is the effective way to balance the NP voltage using the control coefficient ρ . Here will propose a fuzzy controller for the control coefficient ρ , so as to decide ρ intelligently and automatically based on the grade and the trend of the NP imbalance.

Figure 6 gives the fuzzy control block diagram for getting the control coefficient. Figure 7 shows the logical schematic of the fuzzy controller. V_{c1} and V_{c2} are the voltage across the two output capacitor, respectively, e and Δe are the voltage error between the C_1 and the C_2 and the increment of the e . e and Δe are the input variable of the fuzzy controller. ρ is the control coefficient, $\Delta \rho$ is the increment of the control coefficient and also the output variable.

Decision of the precision quantities and quantization:

- With assumption that the scope of the control coefficient is $0.2 < \rho < 0.8$, the scope of the $\Delta \rho$ is $-0.3 < \Delta \rho < 0.3$. The quantization of the $\Delta \rho$ is seen in the Table 2

Hence, the scale factor is: $K_3 = 0.05$

- Considering the NP balanced, the fuzzy controller implements the proportional control as Eq. 4:

$$\Delta \rho = k_D e \tag{4}$$

where, K_D is the proportional coefficient, K_D should be chosen to make the error voltage between the two capacitors smaller and 5 V here. Then K_D can be calculated as the following expression:

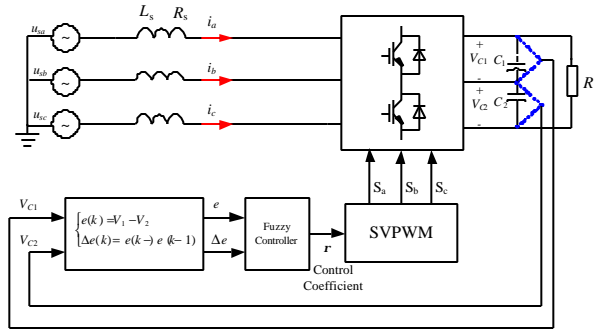


Fig. 6: Block diagram based on fuzzy controller

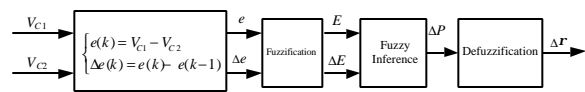


Fig. 7: Logical flow chart for fuzzy controller

Table 2: Quantification of the $\Delta \rho$

Quantification $\Delta \rho$	0	± 1	± 2	± 3	± 4	± 5	± 6
Precision $\Delta \rho$	0	± 0.05	± 0.1	± 0.15	± 0.2	± 0.25	± 0.3

Table 3: Quantification of e

Quantification e	0	± 1	± 2	± 3	± 4	± 5	± 6
Precision e	0	± 0.83	± 1.67	± 2.5	± 3.3	± 4.17	± 5

Table 4: Quantification of Δe

Quantification Δe	0	± 1	± 2	± 3	± 4
Precision Δe	0	± 0.25	± 0.5	± 0.75	± 1

$$K_D = \frac{\Delta \rho}{e_e (\Delta e = 0)} = \frac{0.3}{5} = 0.06 \tag{5}$$

The quantization of the e is seen in the Table 3

- Let $(\Delta e)_m = 1$ V, the quantification of Δe is seen in the Table 4

The quantization factor is: $K_2 = 4$

Fuzzification for error change in error and output variable:

- **Fuzzification for error:** In the universe $[-6, 6]$, seven levels is achieved, i.e., seven fuzzy sets are defined here: PB, PM, PS, ZE, NS, NM, NB. All membership functions for the fuzzy sets choose symmetrical triangles as the Fig. 8. From the Fig. 8, the error to degrees of membership can be gotten as seen in the Table 5
- **Fuzzification for the error in change Δe :** The continue universe $[-4, +4]$ is divided into five levels, i.e., PB, PS, ZE, NS, NB. The membership functions also choose triangles and the error in change to

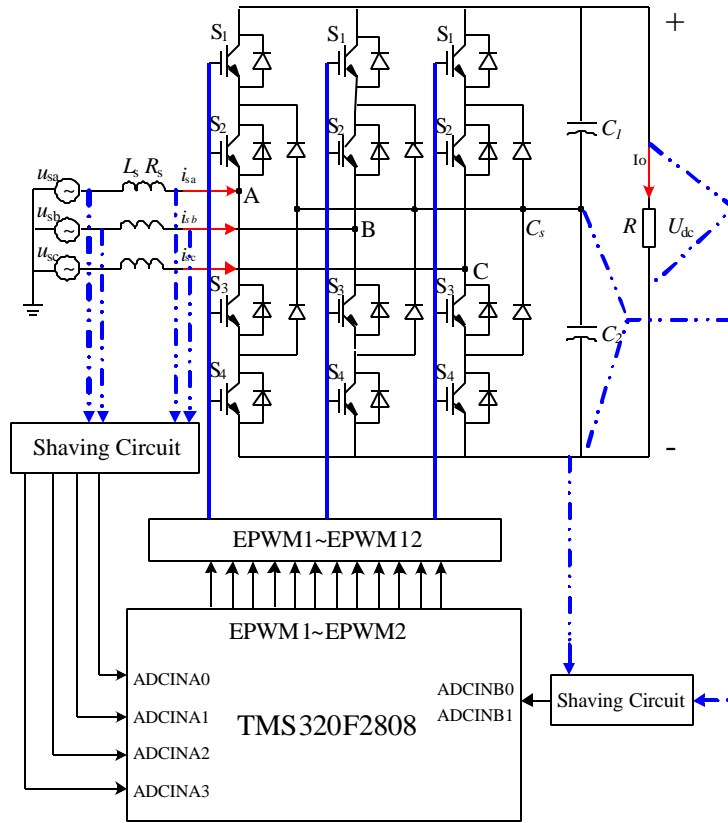


Fig. 8: Control diagram of TL-PWM rectifier based on VOC

Table 5: Degrees of membership for error quantity

E e'	+6	+5	+4	+3	+2	+1	0	-1	-2	-3	-4	-5	-6
PB	1	0.5	0										
PM	0	0.5	1	0.5	0								
PS			0	0.5	1	0.5	0						
ZE					0	0.5	1	0.5	0				
NS						0	0.0	1	0.5	0			
NM									0	0.5	1	0.5	0
NB											0	0.5	1

Table 6: Degrees of membership for change in error

Δe Δe'	+4	+3	+2	+1	0	-1	-2	-3	-4
PB	1	0.5	0						
PS	0	0.5	1	0.5	0				
ZE			0	0.5	1	0.5	0		
NS					0	0.5	1	0.5	0
NB							0	0.5	1

Table 7: Fuzzy control rules

e Δp Δe	PB	PM	PS	ZE	NS	NM	NB
PB	PB	PB	PB	PM	PS	ZE	NM
PS	PB	PB	PM	PS	ZE	NM	NM
ZE	PB	PM	PS	ZE	NS	NM	NB
NS	PM	PM	ZE	NS	NM	NB	NB
NB	PM	PS	NS	NM	NB	NB	NB

degrees of membership by a lookup can be gotten as seen in the Table 6

- **Fuzzification for the output Δp:** Here, the output Δp is proportional to the error e, hence, the fuzzification for the output Δp is the same as that of the error e as seen in the Table 5

Decision of the fuzzy rules: Fuzzy “if e and Δe then Δp” rules is applied. The concrete rules are as follows (Table 7).

- **Defuzzification for Δp:** The resulting fuzzy set must be converted to a number that can be sent to the

process as a control signal. In light of the most and the least inference principle combined with centroid method, the response values are shown in the Table 8. It is clear that the control coefficient level can be achieved only if we know the level about the error and the error in change. As a consequence, the precision value of the control coefficient Δp is accomplished

Table 8: Response values

E\A\B\AE	+6	+5	+4	+3	+2	+1	0	-1	-2	-3	-4	-5	-6
+4	6	6	6	6	5	5	4	3	1	0	0	-2	-3
+3	6	6	6	5	5	4	3	2	1	-1	-1	-2	-3
+2	6	6	5	5	4	3	2	1	0	-2	-3	-4	-4
+1	6	5	5	4	3	2	1	0	-1	-2	-3	-5	-5
0	6	5	4	3	2	1	0	-1	-2	-3	-4	-5	-6
-1	5	5	3	2	1	0	-1	-2	-3	-4	-5	-5	-6
-2	4	4	3	2	0	-1	-2	-3	-4	-5	-5	-6	-6
-3	4	3	2	1	0	-2	-3	-4	-5	-5	-6	-6	-6
-4	4	3	2	0	-1	-3	-4	-5	-5	-6	-6	-6	-6

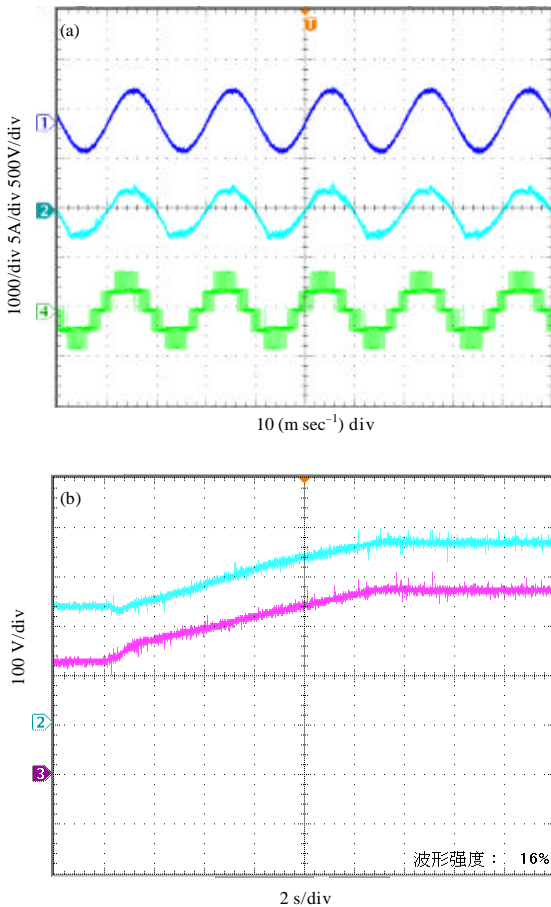


Fig. 9(a-b): Voltage and current waveforms (a) Main waveforms in steady state and (b) The drive signals

EXPERIMENTAL RESULTS

Figure 8 shows the schematic diagram of the system hardware. Its control circuits mainly consist of TI DSP TMS320F2808 and drive circuits. The NP balance at DC side is implemented by software based on fuzzy controller discussed above. Both the voltage and current control loops employ PI regulator calculated in the code [17, 18, 19]. The experimental prototype parameters are as

follows: Input phase-to-phase voltage $E_m = 311$ V, output voltage $U_{dc} = 760$ V, $P_o = 1$ kW, switch frequency $f_s = 20$ KHz, $R_s = 0.002 \Omega$, $L_s = 2$ mH and $C_s = 1000 \mu F$.

The DSP TMS320F2808 is employed; DSP2808 can run at 100 MIPS, so the coordinate transformation, voltage regulator, current regulator, SVPWM algorithm, fuzzy control algorithm and sampling signal process can all be operated at 20 KHz switching frequency. In Fig. 9a, channel 1 and 2 show the phase-to-phase input voltage and input current waveforms, respectively and channel 4 presents the NP voltage waveform between the bridge leg A and B. Figure 9b gives the output voltages across the two capacitors. Channel 1 shows the voltage of C_1 and channel 2 shows the voltage of C_2 , we can conclude the NP voltage between the output capacitors is always balanced both in the stage of start and the steady state due to the NP control strategy based on fuzzy control. The experimental results show: The use of the proposed neutral point balance technique is effective and guarantees three-level PWM rectifier to implement high power factor.

CONCLUSION

The neutral point voltage unbalance affected by large, middle and small vectors is analyzed and only the small vectors can be optimized to balance the neutral point voltage. And a fuzzy-control-based control coefficient for small vector generation is proposed. The NP voltage direction should be judged firstly and then the time duration of the positive and negative small vectors are adapted itself and assigned with control coefficient to control the NP voltage towards balance direction. The method proposed is easy to be implemented in digital control mode and the cost can be cut down without additional current sensor. The balance of the two output capacitors promises the three-level PWM rectifier to be operated with unity power factor.

ACKNOWLEDGMENTS

This study is supported by the National Natural Science Foundation of China (51377083) and the Prospective Research Project of Jiangsu Province (BY2013063-01).

REFERENCES

Chen, Y., X. Gao, Y. Li, Q. Liu and Q. Gao, 2012. An improved SVPWM algorithm with low computational overhead for three-level inverter. Proceedings of the 7th International Power Electronics and Motion Control Conference, Volume 4, June 2-5, 2012, Harbin, China, pp: 2501-2505.

- Cheng, S., Y. Liu and B. Wu, 2008. SVM algorithm of three-level NPC inverter. Proceedings of the 3rd IEEE Conference on Industrial Electronics and Applications, June 3-5, 2008, Singapore, pp: 2194-2198.
- Dou, Z., M. Cheng, S. Li, Z. Ling and X. Cai, 2011. Decoupling control and neutral-point-potential balance control for three-level neutral-point-clamped rectifier. *Electr. Power Autom. Equip.*, 31: 32-37.
- Du, E., L. He, X. Li and Y. Ma, 2010. Neutral point potential balance of three-level inverter based on parameters self-tuning fuzzy logic control strategy. Proceedings of the 36th Annual Conference on IEEE Industrial Electronics Society, November 7-10, 2010, Glendale, AZ., USA., pp: 2863-2867.
- Fan, B., W.G. Zhao, W. Yang and R.Q. Li, 2012. A simplified SVPWM algorithm research based on the neutral-point voltage balance for NPC three-level inverter. Proceedings of the IEEE International Conference on Automation and Logistics, August 15-17, 2012, Zhengzhou, China, pp: 150-154.
- Gong, B., S. Cheng and Y. Qin, 2013. Simple three-level neutral point voltage balance control strategy based on SVPWM. *Archiv. Electr. Eng.*, 62: 15-23.
- Jiang, W.D., Q.J. Wang, Q. Chen and X.F. Shi, 2008. A novel SVPWM method for N level voltage source inverter. *Proc. Chin. Soc. Electr. Eng.*, 28: 12-18.
- Kim, J.Y., M. Kim, S. Lee, J. Oh, K. Kim and H.J. Yoo, 2010. A 201.4 GOPS 496 mW real-time multi-object recognition processor with bio-inspired neural perception engine. *IEEE J. Solid State Circuits*, 45: 32-45.
- Lan, Z., C. Li, Y. Li, C. Zhu and C. Wang, 2011. Development of IGCT-based large power three-level dual-PWM converter. *Trans. China Electrotechn. Soc.*, 26: 36-40.
- Yan, L., W. Xu and X. Yan, 2011. Research based on SVPWM method of three level inverter. Proceedings of the 30th Chinese Control Conference, July 22-24, 2011, Yantai, China, pp: 4513-4515.
- Qu, K., X. Jin, Y. Xing, Z. Ding and W. Chen, 2011. A SVPWM control strategy for NPC three-level inverter. Proceedings of the Power Engineering and Automation Conference, Volume 1, September 8-9, 2011, Wuhan, China, pp: 256-259.
- Rajashekhar, S. and K.P. Vittal, 2010. Novel algorithm for control of a shunt active power filter based on a three-level voltage source inverter. *Acta Techn. CSAV*, 55: 149-162.
- Singh, B. and S. Sharma, 2011. Neural network based voltage and frequency controller for isolated wind power generation. *IETE J. Res.*, 57: 467-477.
- Song, W. and X. Feng, 2011. A single phase SVPWM optimized method. *Trans. China Electrotechn. Soc.*, 26: 107-113.
- Wang, H.X., W.M. Ma, D.L. Zhang, F. Xiao, M.L. Chen and Y. Liu, 2011. SVPWM over-modulation scheme of NPC three-level converter using vector synthesization. *High Voltage Eng.*, 37: 234-240.